# Efficient Room-Temperature Production of High-Quality Graphene by Introducing Removable Oxygen Functional Groups to Precursor

Supporting Information

*Hongwu Chen,[a] Wencheng Du,[a] Jing Liu,[a] Liangti Qu[a,b] and Chun Li*[a]*

[a] Department of Chemistry, MOE Key Laboratory of Bioorganic Phosphorus Chemistry & Chemical Biology, Tsinghua University, Beijing 100084, China.

[b] Key Laboratory for Advanced Materials Processing Technology, Ministry of Education of China; State Key Laboratory of Tribology, Department of Mechanical Engineering, Tsinghua University, Beijing 100084, P. R. China

*Corresponding author E-mail: chunli@mail.tsinghua.edu.cn

## Experimental details.

I. Synthesis of graphene oxide precursor (in details);

II. Fabrication of functional graphene-based assemblies;

III. Characterization details;

IV. Evaluation on the materials performance.

### I. Synthesis of graphene oxide precursor (in details);

**Synthesis of CGO.** Graphite powder (1 g, 325 mesh, dried at 60°C for 24 h) was added to 250 mL flask and followed by the slow addition of concentrated sulfuric acid (30 mL). Then the reaction slurry was vigorously stirred at 20°C for 30 min. After that, potassium permanganate (3.0 g) was added over a period of 10 min and the reaction system was further mixed by mechanical stirrer for another 10 min. The first-step oxidation was performed over 1 h under 35°C and the following second-step oxidation process initiated by the rapid addition of 30 mL $H_2O$ in 10 min and kept at 95°C for 15 min. The reaction was terminated by pouring the reaction system into 500 mL 20°C deionized water and the slow addition of 10 mL 30% $H_2O_2$ to reduce Mn(VII) species.

**Synthesis of GO-20, GO-$P_4O_{10}$ and GO-5.** Graphite powder (1 g, 325 mesh, dried at 60°C for 24 h) was added to 250 mL flask, followed by the addition of concentrated sulfuric acid (30 mL) in the case for GO-20/GO-5 and $P_4O_{10}$ dried $H_2SO_4$ (30 mL) for GO-$P_4O_{10}$. After vigorous stirring at 20°C (for GO-20 and GO-$P_4O_{10}$) or 5°C (for GO-5) over 30 min, potassium permanganate (3.0 g) was added over a period of 10 min. The oxidation process was performed over 3 h under 20°C (for the production of GO-20 and GO-$P_4O_{10}$) or over 12 h under 5°C (for the synthesis of GO-5). After that the reaction was terminated by the same method specified in the preparation of CGO.

**Exfoliation and purification of GO samples.** All graphite oxide samples were separated from the reaction system by centrifugation at 1,000 *g* for 5 min. Then graphite

oxide samples were washed with 1,000 mL 1:10 v/v% HCl solution for 3 times by centrifugation. After washing with deionized water for another 3 times, the graphite oxide dispersion was exfoliated by mild sonication (input energy < 30 J $L^{-1}$ $s^{-1}$) at 20°C for 10 min. After that, the GO dispersion was subjected to another 3 cycles of centrifugation at 1,000 *g* 20 min for each to remove the graphite powder and un-exfoliated graphite oxide agglomerates. Finally, the GO dilute dispersion was concentrated by centrifugation at 10,000 *g* for 1 h, generating the GO stock at solid content up to 2 wt%.

## II. Fabrication of functional graphene-based assemblies;

**Fabrication of GO assemblies.** Fabrication procedures of compact GO films, ultra-light GO aerogels and GO fibers were elaborated in main text. Note that the freezing process of dilute GO dispersion (1.0 mg $mL^{-1}$) for the fabrication of bulk aerogel without defects should be carried out slowly (over > 15 min freezing time for the processing of 50 mL GO dispersion).

**Reduction of GO assemblies.** Reduction of compact GO films was performed by soaking the film materials in HI acid (15 wt%) at room-temperature over a period of 12 h. Then the reduced GO films were washed with ethanol for 24 h to remove the adsorbed $I_2$.

## III. Characterization details;

**Sampling of monolayer GO on mica or $SiO_2$/Si substrate.** For the measurements on size and shape distribution and thickness of GO flakes, high-quality SEM images of GO sheets assembled on $SiO_2$/Si surface and AFM images obtained from the GO on mica surface were required. Herein, the sampling process was carried out by dripping diluted GO-ethanol suspension (0.01 mg $mL^{-1}$) onto the $SiO_2$/Si substrate (with 300 nm thick $SiO_2$ on n-doped Si wafer, cleaned by sonication in ethanol) and by dripping GO-

water suspension (0.02 mg $mL^{-1}$) onto freshly cleaved mica surface followed by drying for 48 h prior to AFM characterization.

**$L_D$ derived from Raman characterization.** Raman characterization was conducted on monolayer rGO sheets assembled on $SiO_2$/Si surface (reduced from GO monolayer, discussed in main text). According to the previous works[1–3], the statistical results for $I_D/I_G$ were closely related to the average distance between structural defects ($L_D$) on graphene basal plane. Furthermore, for rGO monolayer samples prepared from chemically oxidized GO precursor, the relationship between $L_D$ and $I_D/I_G$ was shown to follow the formula below[3]:

$$\frac{I_D}{I_G} = f(E_L) \times \frac{r_A^2 - r_S^2}{r_A^2 - 2r_S^2} \times \left( e^{-\frac{\pi r_S^2}{L_D^2}} - e^{-\frac{\pi(r_A^2 - r_S^2)}{L_D^2}} \right) \quad (1)$$

In which $f(E_L)$ is the parameter related to the energy of laser (eV) used for Raman characterization and specified by $f(E_L) = 160E_L^{-4}$. $r_A$ and $r_S$ are the radius of the area enclosing the point defect and the area of point defect, respectively, they were set to 3.1 nm and 1 nm in this model. Then the specific formula for the calculation of $L_D$ through $I_D/I_G$ value was obtained below:

$$\frac{I_D}{I_G} = 6.08 \times \left( e^{-\frac{\pi}{L_D^2}} - e^{-\frac{8.61\pi}{L_D^2}} \right) \quad (2)$$

**Determination of water content in commercial concentrated $H_2SO_4$ used in this study.** Water content in commercial concentrated sulfuric acid was determined by acid-base titration method. NaOH solution (~ 0.1 M) was calibrated by potassium hydrogen phthalate, employing phenolphthalein as pH indicator, for at least three parallel experiments that displayed standard deviation < 4‰. Then the diluted $H_2SO_4$ was titrated by NaOH solution, and the water content in concentrated $H_2SO_4$ was obtained by the formula below:

$$\text{Water content (wt\%)} = \left( 1 - \frac{m(\mathrm{H_2SO_4}\ \textit{determined by titration})}{m(\textit{conc.}\,\mathrm{H_2SO_4})} \right) \times 100\% \quad (3)$$

## IV. Evaluation on the materials performance.

**Comparison of graphene synthesis method in terms of the energy-efficiency and materials performance.** The production of high-quality graphene in an energy-efficient way was constantly explored. Herein the methodology that involves the production of graphene oxide precursor and the reduction process was used and we carried out comparison analysis on the energy-efficiency and the structural integrity of final graphene film materials based on the existed reports. Energy-efficiency is reflected in the energy-yield index (EI), which is defined below:

$$\mathrm{EI} = \frac{E(cooling) + E(hydrolysis)}{\eta \times 1J} \Big/ \frac{1000 \times t(h)}{Yield(\%) \times 1h} \tag{4}$$

in which E(cooling) represents the energy needed to cooling down the reaction slurry to particular temperature and E(hydrolysis) is the heat generated through the second-oxidation process (if available). The expressions of which are shown below:

$$E(cooling) = (298 - T_{end}) \times \rho V_{H_2SO_4} C_p \tag{5}$$

$$E(hydrolysis) = 4.61 \times \frac{n_{H_2O} \times V_{H_2SO_4}}{n_{H_2O} \times \frac{M_r(H_2SO_4)}{30} + 1.7983} \tag{6}$$

$T_{end}$ represents the temperature at the point oxidants were added (e.g., 278 K in the synthesis of GO-5). $C_p$ is the molar heat capacity of pure $H_2SO_4$ at constant pressure. All the thermodynamics constants and the calculation of differential heat of dilution (E(hydrolysis)) were referred to literature[4].

In addition, the heat transfer efficiency was influenced by the temperature difference between the system and environment, henceforth we introduced $\eta$, defined below:

$$\eta = \frac{T_{end}}{298.15 - T_{end}} \tag{7}$$

$\eta$ represents the maximum cooling efficiency regarding the system as a reverse Carnot heat engine. In our model, the heat transfer (i.e., heat conduction, convection and radiation) between the reaction system and environment was not considered—in the actual production process, the energy loss could be corrected in $\eta$.

**Mechanical and conductivity test.** The mechanical test was performed according to the standard determination of tensile properties of thin plastic sheeting[5]. The sample strips (with length > 25mm and width = 3.0 mm) were prepared by cutting GO films with razor blade. After that, tensile test was conducted on universal mechanical testing machine (Instron 3342, USA). The loading rate was set to 0.3 mm $min^{-1}$ and the grip separation was 15.0 mm. Sheet resistance of rGO films were recorded by a four-point probe on the surface. The thickness of GO/rGO film was obtained from the SEM images of cross-section of each sample strip.

**Fabrication of EDLC and the performance.** Schematic illustration of the device structure of EDLC that employed rGO films as flexible current collector is shown in **Figure S9**a. The activated carbon electrode was composed of 80 wt% activated carbon (active materials), 10 wt% Super P carbon black powder (conductive materials) and 10 wt% PTFE binder. 1.0 M $H_2SO_4$ was used as the electrolyte. Cyclic voltammetry and electrochemical impedance spectroscopy (EIS) tests were performed and the results were recorded in **Figure 5**c and **Figure S9**.

## Supplementary figures and tables.

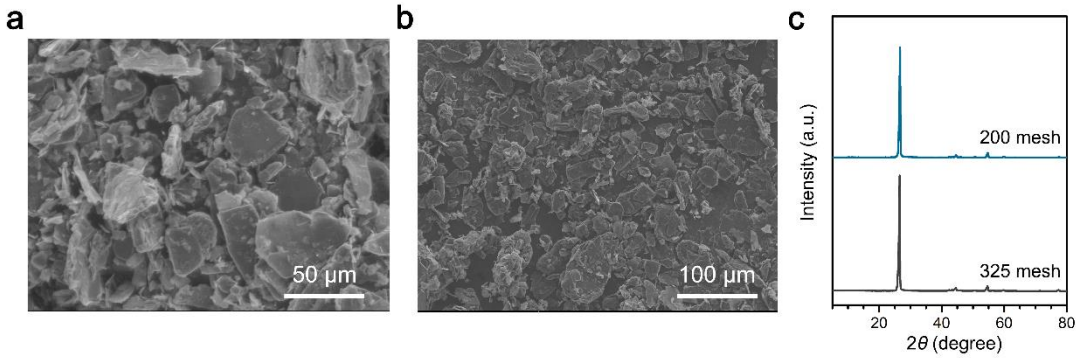


**Fig. S1** Characterization of graphite powders. SEM image of (a) 325 mesh and (b) 200 mesh graphite powder; (c) XRD patterns.

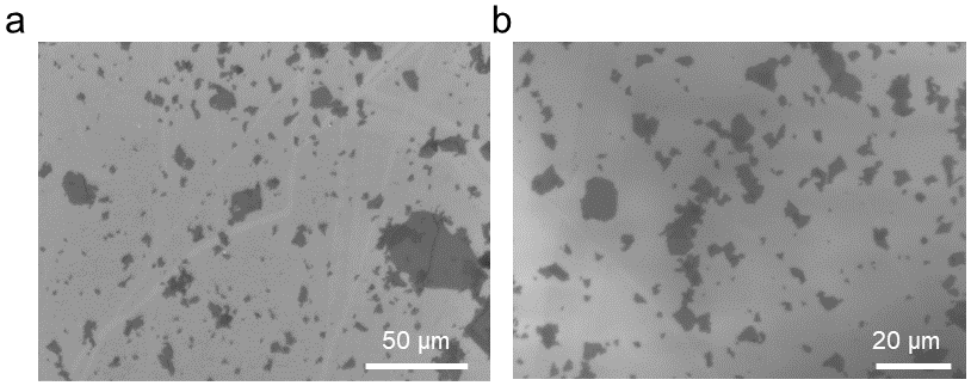


**Fig. S2** SEM images of (a) CGO and (b) GO-5 flakes.

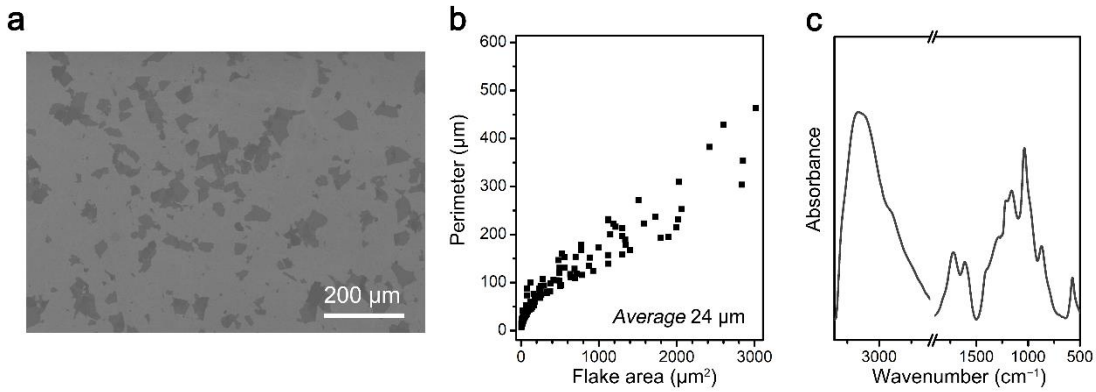


**Fig. S3** Characterization of 200 mesh GO prepared by the room-temperature method. (a) SEM image; (b) Plot of perimeter against flake area of GO sheets; (c) FT-IR characterization. The results indicated that the method proposed in this study could also be used in the synthesis of large graphene flakes.

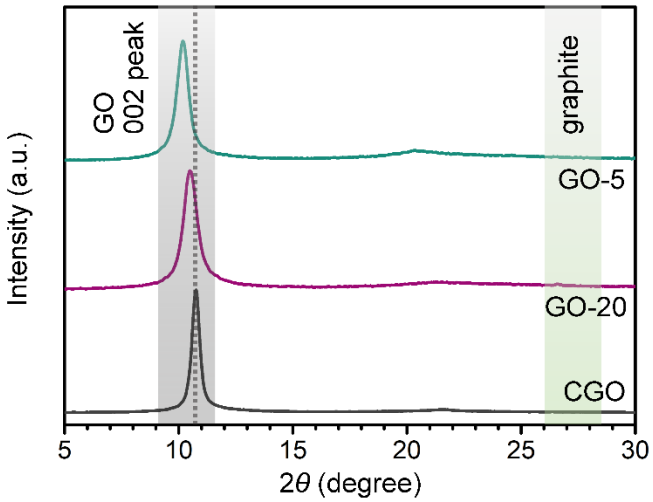


**Fig. S4** XRD patterns of CGO, GO-20 and GO-5 films, showing the complete removal of graphite phase. Besides, the larger d-spacings and more disordered structure (from the larger FWHM of GO 002 peak) of GO-20 and GO-5 films result from the higher organosulfate species content[6] (**Table S1**).

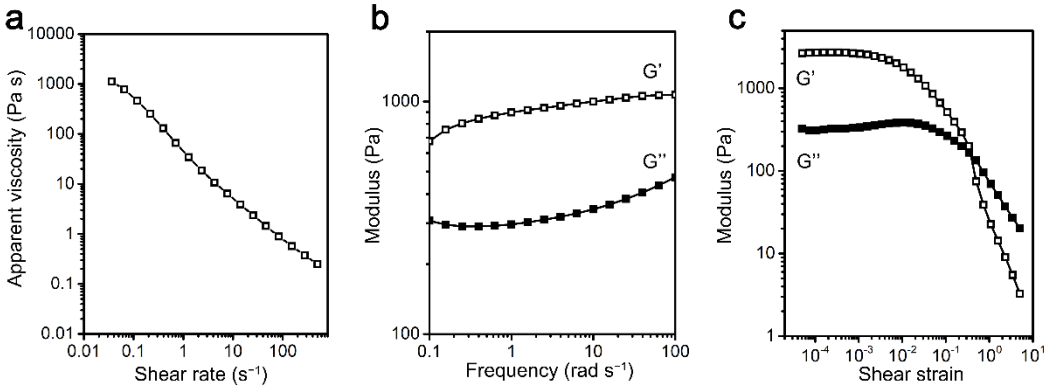


**Fig. S5** Rheology behavior of GO-20 aqueous dispersion (2 wt%). The excellent dispersibility of GO-20 sample makes it possible to form a highly sticky, 3D printable ink[7] with elastic modulus up to 2,800 Pa and G'/G'' value up to 4.6.

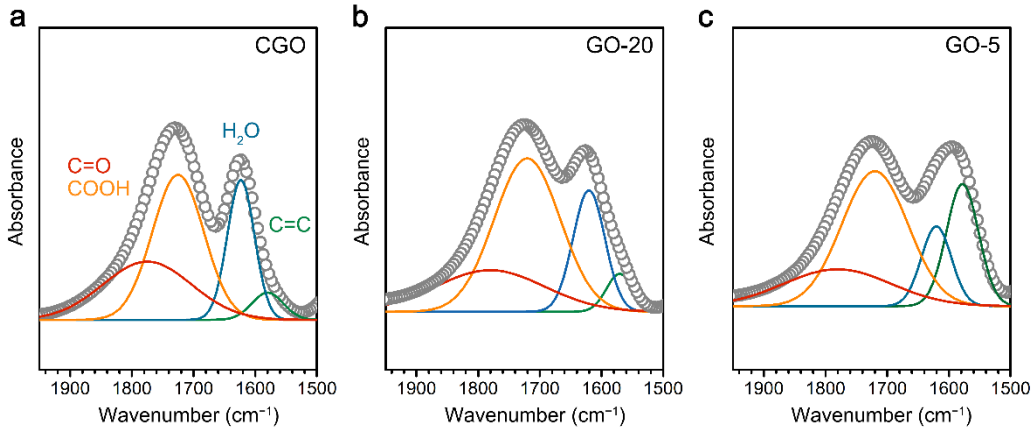


**Fig. S6** Deconvolution of FT-IR absorbance band in the range of 1500 ~ 1900 $cm^{-1}$ of (a) CGO, (b) GO-20 and (c) GO-5 samples, showing the difference in the relative proportion of C=C conjugated area and carbonyl/carboxyl groups.

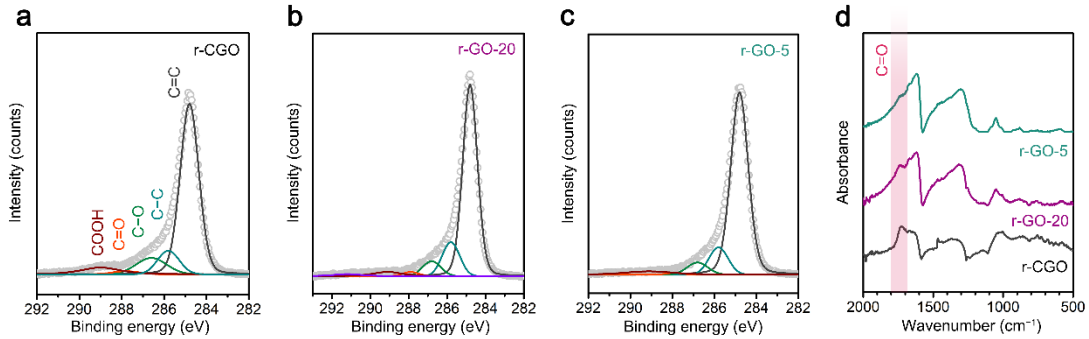


**Fig. S7** Characterization on the chemical structure of rGO films reduced by HI acid from GO films. (a-c) C 1s XPS spectra of r-CGO, r-GO-20 and r-GO-5 samples, respectively; (d) FT-IR spectra. From these results, r-CGO samples showed higher content of carboxyl groups, which was inherited from the more defective GO precursor.

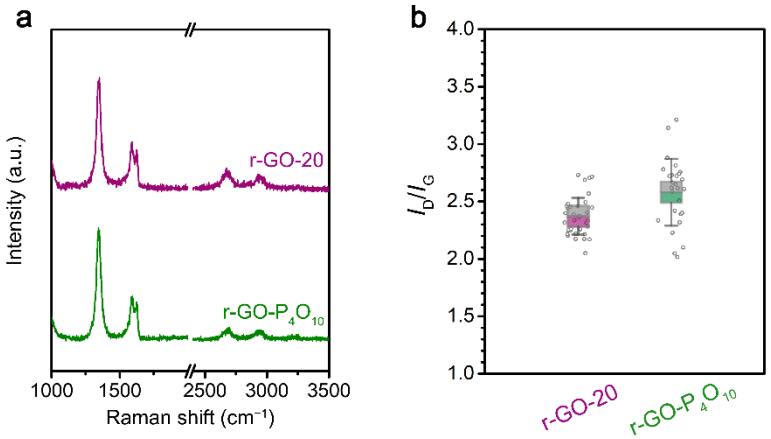


**Fig. S8** Raman characterization on the structural integrity of rGO monolayers reduced by HI vapor: (a) r-GO-20 and (b) r-GO-$P_4O_{10}$. The higher $I_D/I_G$ value for r-GO- $P_4O_{10}$ samples suggested the better structural integrity.

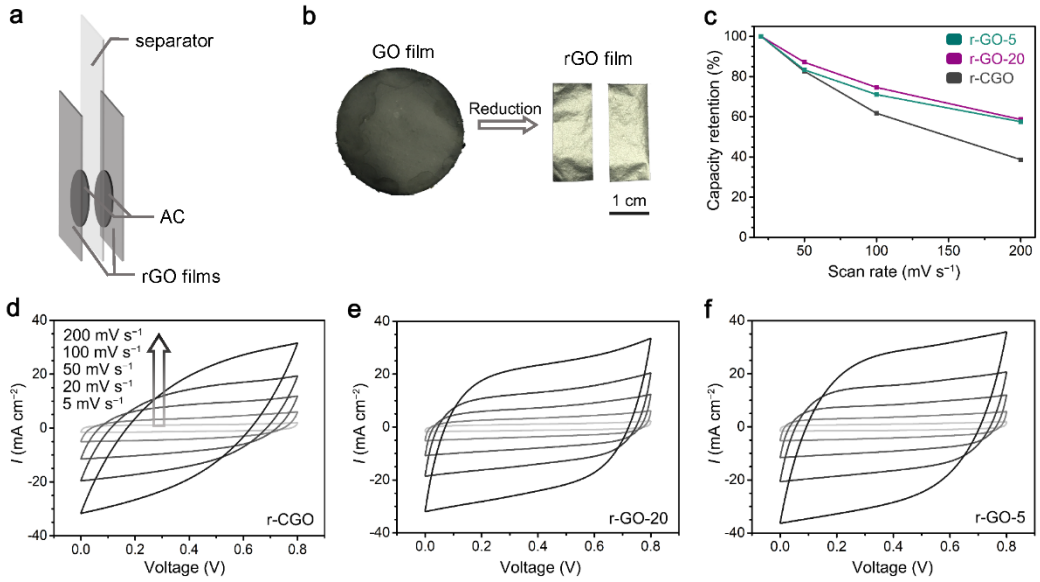


**Fig. S9** Fabrication of EDLC employing rGO film as the current collector and the related electrochemical performance. (a) Schematic illustration of the device structure; (b) The fabrication process of rGO films; (c) Capacity retention of EDLCs under increased scan rate using different rGO films as current collector; (d-f) cyclic voltammetry tests of EDLCs (operated in 1.0 M $H_2SO_4$).

**Table S1.** Statistics of XPS characterization on GO and rGO samples.

| **Chemistry** | C/O at. ratio* | COOH (%) | S (at%) |
|---|---|---|---|
| CGO | 2.0 | 3.1 | 1.5 |
| GO-20 | 2.1 | 1.3 | 3.2 |
| GO-5 | 2.4 | 1.4 | 3.9 |

*derived from the atomic % results for a normal XPS survey;

**Table S2.** Statistics of Raman characterization on rGO monolayers.

| **Raman results** | $I_D/I_G$ | $\Gamma_{2D}$ ($cm^{-1}$) | G position ($cm^{-1}$) |
|---|---|---|---|
| r-CGO | 1.78 ± 0.16 | 144 ± 26 | 1591.2 ± 2.6 |
| r-GO-20 | 2.37 ± 0.16 | 88 ± 13 | 1589.9 ± 2.1 |
| r-GO-5 | 2.55 ± 0.16 | 78 ± 12 | 1589.5 ± 1.9 |

## References for SI.


(S1) Ferrari, A. C.; Meyer, J. C.; Scardaci, V.; Casiraghi, C.; Lazzeri, M.; Mauri, F.; Piscanec, S.; Jiang, D.; Novoselov, K. S.; Roth, S.; Geim, A. K., Raman spectrum of graphene and graphene layers. *Phys. Rev. Lett.* **2006,** *97*, 187401.

(S2) Lucchese, M. M.; Stavale, F.; Ferreira, E. H. M.; Vilani, C.; Moutinho, M. V. O.; Capaz, R. B.; Achete, C. A.; Jorio, A., Quantifying ion-induced defects and Raman relaxation length in graphene. *Carbon* **2010,** *48*, 1592−1597.

(S3) Cancado, L. G.; Jorio, A.; Martins Ferreira, E. H.; Stavale, F.; Achete, C. A.; Capaz, R. B.; Moutinho, M. V. O.; Lombardo, A.; Kulmala, T. S.; Ferrari, A. C., Quantifying defects in graphene via Raman spectroscopy at different excitation energies. *Nano Lett.* **2011,** *11*, 3190−3196.

(S4) Louie, D. K., Handbook of sulphuric acid manufacturing, 2nd edition. DKL Engineering Inc.: Thornhill, Ontario, 2008.

(S5) ASTM D882-12, Standard test method for tensile properties of thin plastic sheeting, ASTM International, West Conshohocken, PA, 2012. http://www.astm.org.

(S6) Zhang, M.; Wang, Y.; Huang, L.; Xu, Z.; Li, C.; Shi, G., Multifunctional pristine chemically modified graphene films as strong as stainless steel. *Adv. Mater.* **2015**, *27*, 6708−6713.

(S7) Naficy, S.; Jalili, R.; Aboutalebi, S. H.; Gorkin III, R. A.; Konstantinov, K.; Innis, P. C.; Spinks, G. M.; Poulinc, P.; Wallace, G. G., Graphene oxide dispersions: tuning rheology to enable fabrication. *Mater. Horiz.* **2014**, *1*, 326−331.